https://doi.org/10.1021/jm501420k

Novel Antitumor Cisplatin and Transplatin Derivatives Containing 1-Methyl-7-Azaindole: Synthesis, Characterization and Cellular Responses

Jitka Pracharova,[†] Teresa Saltarella,[‡] Tereza Radosova-Muchova,[†] Simone Scintilla,[‡] Vojtech Novohradsky,[§,II] Olga Novakova,[§] Francesco P. Intini,[‡] Concetta Pacifico,[‡] Giovanni Natile,[‡] Petr Ilik,[†] Viktor Brabec,[II] and Jana Kasparkova*[,§]

[†] Department of Biophysics, Centre of the Region Hana for Biotechnological and Agricultural Research, Palacky University, Slechtitelu 11, 783 41 Olomouc, Czech Republic
[‡] Department of Pharmaceutical Chemistry, University of Bari, 70125 Bari, Italy
[§] Institute of Biophysics, Academy of Sciences of the Czech Republic, v.v.i., Kralovopolska 135, CZ-61265 Brno, Czech Republic
[II] Department of Biophysics, Faculty of Science, Palacky University in Olomouc, Slechtitelu 11, 78371 Olomouc, Czech Republic

ABSTRACT:

Two new platinum(II) bifunctional compounds, having cis- and trans- geometry and containing the 1-methyl-7-azaindole ligand, have been synthesized, fully characterized, screened for their toxicity against cancer and nontumorigenic cell lines, evaluated for their efficiency to enter the cells, damage DNA, affect cell cycle, and induce apoptosis. When compared to conventional cisplatin, substitution of 1-methyl-7-azaindole for ammine results in an increase of the toxic efficiency particularly in cisplatin-resistant cancer cells, the cytotoxicity being comparable for both the cis- and trans-isomers. The ability to overcome resistance to cisplatin appears to be associated with an increased level of DNA platination by these compounds as compared to cisplatin. For both isomers the cytotoxic effect is accompanied by triggering of apoptosis and cell cycle arrest in S and G_2/M phases. Interestingly, whilst the trans isomer demonstrates its biological action in the early phases of the treatment, the cytotoxic effect of the cis isomer is more pronounced after longer incubation times. Notably, for both isomers it is possible to detect the accumulation and distribution in living cells by confocal microscopy.

INTRODUCTION

Cisplatin [*cis*-diamminedichloridoplatinum(II)] and other platinum-based anticancer agents are well known to be effective in the treatment of many human malignancies. However, the ultimate success of these agents is often limited by the natural or acquired drug resistance and side effects. These drawbacks have fostered the search for new antitumor platinum-based drugs with fewer side effects and more effective outcomes. New mononuclear bifunctional platinum drugs have been derived from cisplatin by replacing one or both ammine groups with other nonleaving N-donor ligands. The design of such derivatives has been inspired by the observation that the carrier ligands can deeply affect the pharmacological behavior of the

drug including cell accumulation and distribution, activation, DNA binding, and cellular responses to the DNA damage. In other words, nonleaving ligands of cisplatin derivatives can modulate their biological properties.[1-4]

Some of us have shown in recent papers[5, 6] that replacement of the ammine ligands of cisplatin by 7-azaindole derivatives results in considerable enhancement of cytotoxicity against several human cancer cell lines. Thus, the rational chemical design can be applied also to this class of compounds since key substituents at the 7-azaindole ring system can play a major role in controlling the chemical and biological properties, such as cellular accumulation and distribution, effects at the level of cell cycle regulation, propensity for DNA adduct repair, binding to DNA, and reactivity toward sulfur-containing nucleophiles. Hence, substituted 7-azaindoles can offer a good opportunity for the synthesis of novel therapeutic agents.

The rational design of novel platinum anticancer drugs can also benefit from early information on the trafficking and localization of platinum drugs in tumor cells. Therefore, confocal microscopy has been successfully applied to investigate the cellular distribution of Pt complexes. However, this relatively simple detection technique, which enables the visualization of compounds in living cells, requires the use of drugs which, after illumination, emit radiation detectable with sufficiently sensitive detectors. Cisplatin and most Pt anticancer complexes do not possess this property and need to be modified with an optically active tag, which, however, can affect its chemical properties and consequently its biological effects. Hence, in order to obtain significant information about the *in vivo* trafficking and localization of a platinum drug in living tumor cells, the modified platinum complex must be as similar as possible to the real drug.

Several attempts have been made to obtain high-resolution images of the cellular accumulation and subcellular distribution of fluorescein-tagged Pt(II) complexes (see Refs.[7-9] as examples). Interestingly, derivatives of cisplatin and transplatin [*trans*-diamminedichloridoplatinum(II)] with one ammine and one aromatic N-donor heterocycle (L) (*cis*- and *trans*-[$PtCl_2(NH_3)L$]) have proved to be endowed with good antitumor activity and one of these compounds, picoplatin [*cis*-amminedichlorido(2-methylpyridine)platinum(II)], is under advanced clinical trials with changing fortunes.[10, 11] This opened the possibility to use a N-donor heterocycle which is intrinsically fluorescent, such as 7-azaindole,[12] for monitoring the cell permeation and distribution of the platinum drugs. However, coordination to platinum results in almost complete quenching of the fluorescence. In addition, 7-azaindole exhibits a pH-dependent fluorescence. Hence, since the pH is different in different cellular compartments, the use of a probe, whose fluorescence is dependent on pH, appears disadvantageous. The latter drawback can be circumvented by derivatization of 7-azaindole with a methyl group.

In the present work we investigate the cytotoxic potential and molecular and cellular pharmacology of two new cisplatin derivatives bearing a nonleaving 1-methyl-7-azaindole ligand (hereafter called 1M7AI). We report the synthesis and characterization of both the cis- and trans-isomers of [$PtCl_2(NH_3)$(1M7AI)] (**1** and **2**, respectively, Figure 1), the crystal structure of **1**, and several biological properties, such as cytotoxicity, impact on cell cycle regulation, and triggering of apoptosis. Moreover, the optical properties were utilized to follow the cellular internalization and distribution of the complexes in tumor cells.

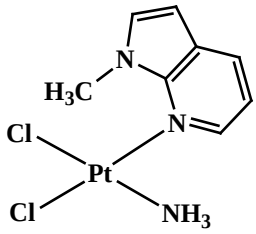

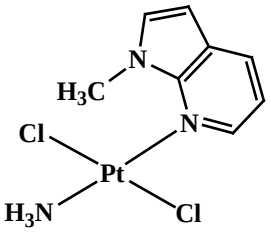

cis-[$PtCl_2(NH_3)$(1M7AI)] (**1**) *trans*-[$PtCl_2(NH_3)$(1M7AI)] (**2**)

Figure 1. Sketch of the molecular structures of *cis*-[$PtCl_2(NH_3)$(1M7AI)] (**1**) and *trans*-[$PtCl_2(NH_3)$(1M7AI)] (**2**) used in this work; 1M7AI = 1-methyl-7-azaindole.

RESULTS AND DISCUSSION

Synthesis and Characterization of the Platinum Complexes. The Pt(II) complexes under investigation have one ammine and one N-donor aromatic heterocycle (1M7AI). For comparison, both the *cis*- and *trans*-[$PtCl_2(NH_3)$(1M7AI)] isomers were synthesized and fully characterized.

The cis complex, *cis*-[$PtCl_2(NH_3)$(1M7AI)] (**1**), was prepared according to a previously reported procedure for the synthesis of analogous compounds,[12, 13] with some modifications. Starting from $K[PtCl_3NH_3]$,[12] the reaction with 1M7AI leads to substitution of one of the two trans chlorides (both cis to the ammine) which are mutually trans-labilized. The reaction is quite slow at room temperature (complete in 4 days) and affords the desired product in moderate yield, the main side-product being the cationic species $[PtCl(NH_3)(1M7AI)_2]Cl$ that can be easily removed (Scheme 1).

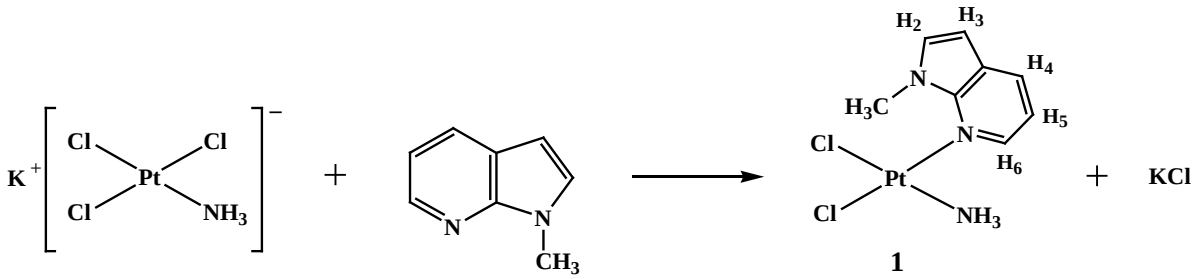

Scheme 1

The synthesis of the trans complex, *trans*-[$PtCl_2(NH_3)$(1M7AI)] (**2**), requires a different procedure in which *cis*-[$PtI_2(NH_3)_2$] is first converted to *cis*-$[Pt(H_2O)_2(NH_3)_2]^{2+}$ (reaction with $AgNO_3$) and then to *cis*-$[Pt(NH_3)_2(1M7AI)_2]^{2+}$ (reaction with 1M7AI. 1:2 ratio). Treatment with excess KI – a ligand with strong trans-labilizing effect – leads to substitution of two trans ligands (one ammine and one 1M7AI) and formation of *trans*-[$PtI_2(NH_3)$(1M7AI)]. The diodido species can be converted to the dichlorido species **(2**) by reaction with $AgNO_3$ (1:2 molar ratio) in water solution followed by addition of excess KCl (Scheme 2).

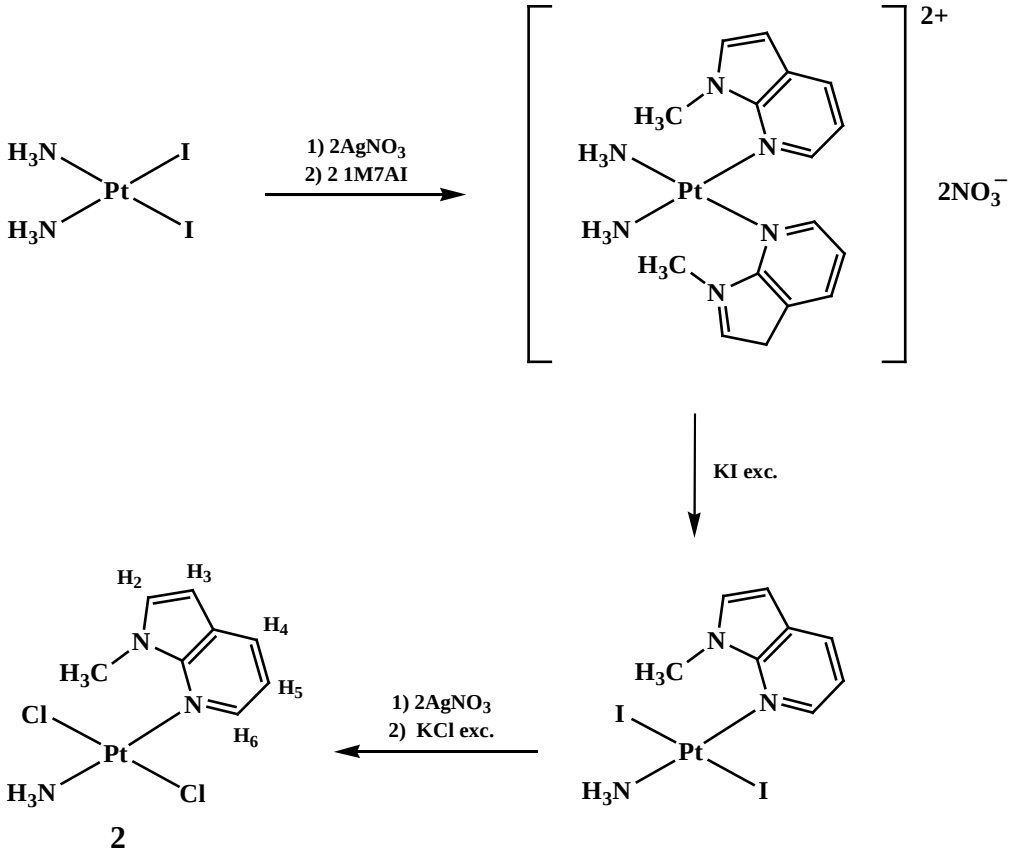

Scheme 2

Both **1** and **2** were characterized by elemental analysis, ESI-MS, and ^{1}H and ^{195}Pt NMR spectroscopy. The ^{1}H-spectra of both compounds show five signals between 9 and 6.5 ppm belonging to aromatic protons, one singlet close to 5.2 ppm belonging to the methyl group, and one broad signal close to 4.0 ppm belonging to the amminic protons. In general, protons are more shielded in the *trans* than in the *cis* isomer. It is noteworthy the remarkable downfield shift ($\Delta\delta > 1.30$ ppm) of the methyl protons upon coordination of 1M7AI to platinum which witnesses the closeness of the methyl group to the deshielding cone originated by the platinum quadrupole in the direction perpendicular to the coordination plane. The assignment of individual aromatic protons was accomplished by 2D COSY experiments (Figure 2, see Schemes 1 and 2 for the numbering of protons).

The coordination of 1M7AI to platinum via N7 causes a $^{3}J_{H6,Pt}$ coupling which is greater for **1** (1M7AI *trans* to Cl, $^{3}J_{H6,Pt} = 41$ Hz) than for **2** (1M7AI *trans* to NH_3, $^{3}J_{H6,Pt} = 32$ Hz) indicating that the ligand trans to 1M7AI has a better σ-donor ability in **2** (NH_3) than in **1** (Cl^-). These results are in full agreement with literature data,[14] and fully support the assignment of the isomer configurations (*cis* or *trans*). The ^{195}Pt chemical shifts were nearly coincident for **1** and **2** (–1,970 and –1,967 ppm, respectively) and fall in the range found for analogous compounds with N_2Cl_2 set of donor atoms.[15] It is interesting to note that also the methyl protons of 1M7AI are coupled with platinum ($^{5}J_{H,Pt} = 10$ Hz) (Figure 3). A similar through space coupling has been observed in few other cases.[16-18] That this is a clear case of through-space coupling is also witnessed by the absence of detectable coupling between Pt and H_5 which are separated by four bonds, one less than the 1-Me protons.

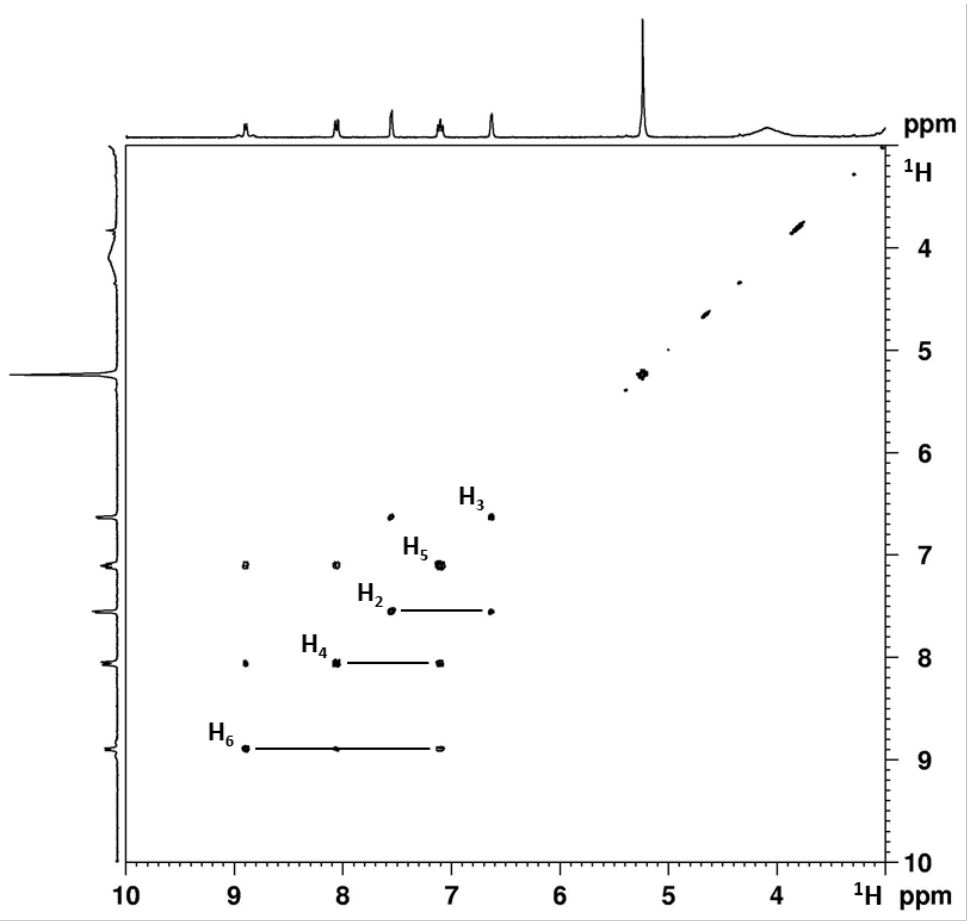

Figure 2. 1D and 2D COSY ^{1}H NMR spectra of *cis*-[$PtCl_2(NH_3)$(1M7AI)] (**1**) in acetone-d_6.

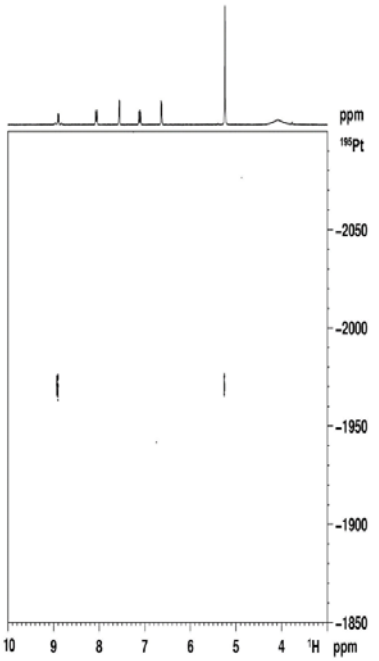

Figure 3. [^{1}H-^{195}Pt] HSQC spectrum of *cis*-[$PtCl_2(NH_3)$(1M7AI)] (**1**) in acetone-d_6 showing the cross peaks between Pt and the H6 (8.89 ppm) and 1-Me (5.24 ppm) protons.

X-ray Structure. An ORTEP drawing of the X-ray structure of complex **1** is shown in Figure 4A, selected bond lengths and angles are given in Table 1.

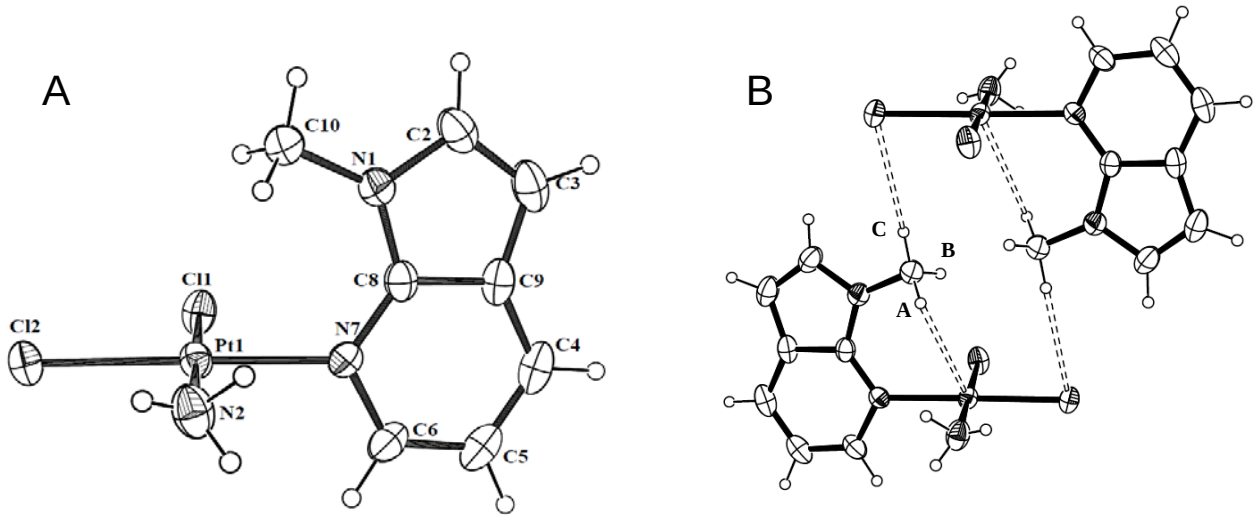

Figure 4. A. ORTEP drawing of the *cis*-[$PtCl_2(NH_3)$(1M7AI)] (**1**) molecule, showing the atomic numbering scheme. The ellipsoids enclose 30% probability. B. ORTEP drawing of a dimeric aggregate of *cis*-[$PtCl_2(NH_3)$(1M7AI)] (**1**) linked by hydrogen bonds.

The Pt atom has the expected square planar coordination geometry, and the donor atoms are two chlorides and two nitrogens in cis positions. The 1M7AI ligand is planar, and his plane is nearly perpendicular to that of coordination [dihedral angle of 82.2(1)°] so to minimize steric interactions with cis ligands.

The platinum-ligand distances (2.045[7] Å for Pt−N and 2.300[2][19] Å for Pt−Cl) are in good agreement with values found in structurally related complexes.[20, 21] The C−N and C−C distances in the heteroaromatic ligand are in accord with an extensive π-bond delocalization.[22] The complex displays a very short platinum-methyl distance [Pt···C(10) distance of 3.203(8) Å]; moreover one methyl proton is directed toward the platinum atom indicating a H-bond type interaction [Pt···H(C) distance of 2.78(9) Å with a Pt···H–C angle of 105°], as confirmed by the downfield shift of the methyl protons with respect to the uncoordinated ligand. In previous reports, similar M···H–C interactions for d^8 square–planar complexes have been described as anagostic interactions.[23] The same methyl forms a hydrogen bond with the chloride of another complex unit related by an inversion center (Figure 4B). Within the dimeric aggregate, two methyl groups are placed at very short distance [C8···C8(-*x* + 1, -*y*, -*z*+1) distance of 3.11(1) Å)], much shorter than the sum of the van der Waals radii (3.40 Å).[24] Others C···C distances shorter than the sum of van der Waals radii have been found for methyl groups in the IsoStar database.[25] However in those cases (three) the C···C distances were longer (between 3.2 and 3.3 Å) than in the present case.[26-28]

Table 1. Selected Bond Lengths (Å) and Angles (°) for *cis*-[$PtCl_2(NH_3)$(1M7AI)] (1)

Pt1−N7	2.043(6)	N7− Pt1−N2	92.2(2)
Pt1−N2	2.047(4)	N2−Pt1−Cl2	88.5(2)
Pt1−Cl1	2.297(2)	N7−Pt1−Cl1	87.7(2)

Pt1−Cl2	2.304(2)	Cl2−Pt1−Cl1	91.57(5)
N7−C6	1.348(7)	C6−N7−Pt1	117.6(4)
N7−C8	1.337(7)	N7−C8−N1	128.1(5)
N1−C8	1.360(7)	N7−C8−C9	123.8(5)
N1−C2	1.382(8)	N1−C8−C9	108.1(5)
N1−C10	1.445(8)		

The H atoms of the methyl group (found in the difference Fourier map) exhibit N−C−H angles smaller than 109° (N1−C10−H10A, N1−C10−H10B, and N1−C10−H10C angles of 104°, 108°, and 104°, respectively), arguably connected to H-bond formation (HA and HC) and short C10···C10 distance.

Intermolecular interactions between amminic groups and chlorido ligands of different molecular units (the chlorido not involved in interaction with the Me of 1M7AI) support the growth of the supramolecular assembly of complex molecules [N2···Cl1(*x* + ½, -*y*+ ½, -*z*+ 1) 3.388(7) Å, (N2)H22···Cl1(*x* + ½, -*y*+ ½, -*z*+ 1) 2.82(9) Å, N2−H22···Cl1(*x* + ½, -*y*+ ½, -*z*+ 1) 143(9)°; N2···Cl1(-*x* + ½+1, *y* - ½, *z*) 3.408(7) Å, (N2)H23···Cl1(-*x* + ½+1, *y* - ½, *z*) 2.69(9) Å, N2−H23···Cl1 (-*x* + ½+1, *y* - ½, *z*) 139(9)°]. In Figure 5 a centrosymmetric tetrameric aggregate of four subunits is shown. In each tetrameric aggregate there are two non-classical C−H···π–C2−C3 contacts [distance between (C)H and π–C2−C3 centroid of 2.65 Å].

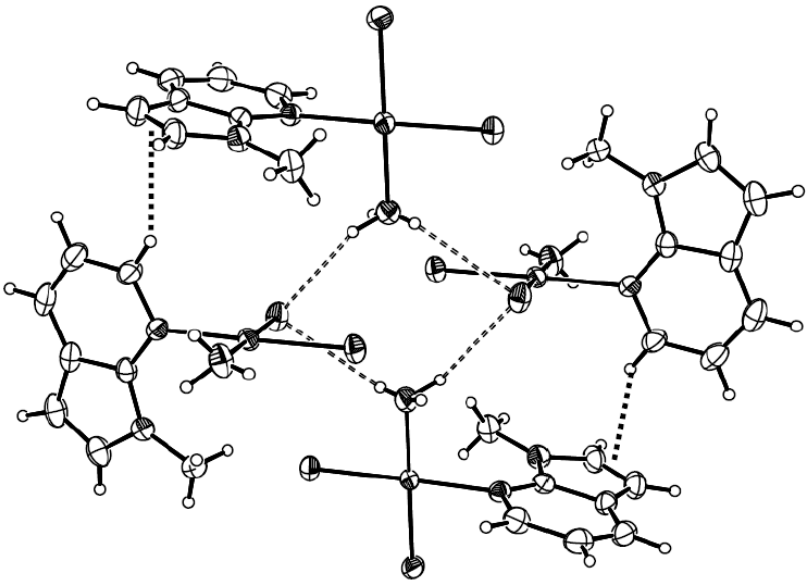

Figure 5. ORTEP drawing of a centrosymmetric tetrameric aggregate of *cis*-[$PtCl_2(NH_3)$(1M7AI)] (**1**) linked by hydrogen bonds and showing CH···π–C2−C3 interactions.

Cytotoxicity. The cytotoxic activity of **1** and **2** was determined against human ovarian carcinoma cell lines A2780 (cisplatin sensitive) and A2780cisR (with acquired resistance to cisplatin) and human breast adenocarcinoma cells MCF-7 (inherently resistant to cisplatin) commonly used to test cytotoxic activity of cisplatin derivatives and other antitumor metallodrugs. The tumor cell lines were incubated with the platinum compounds and cell survival in cultures was evaluated as described in the "Experimental section". The IC_{50} values

(concentration of compound which causes death in 50 % of cells) for 72 h of treatment are reported in Table 2; both compounds showed promising activity

Table 2. Cytotoxicity [IC_{50} Mean Values (μM)] Obtained for 1, 2 and Cisplatin (72 h Incubation Time)[a]

	A2780	A2780cisR	MCF-7	Human primary skin fibroblasts
Cisplatin	2.38 ± 0.12	15.58 ± 0.06 (6.5)	30.01 ± 1.20	68.98 ± 0.87
1	4.20 ± 0.16	4.30 ± 0.52 (1.0)	14.01 ± 2.02	51.19 ± 2.35
2	3.61 ± 0.11	2.78 ± 0.64 (0.77)	12.24 ± 2.44	17.13 ± 2.90

[a]The experiments were performed in triplicate. The results are expressed as mean values ± SD of three independent experiments. Resistance factor, defined as IC_{50}(resistant)/IC_{50}(sensitive), is given in parentheses.

In cisplatin-sensitive A2780 cells, the activity of **1** and **2** was comparable to that of cisplatin. Importantly, both compounds were markedly more toxic than cisplatin in cisplatin-resistant A2780cisR cells and also moderately more toxic in MCF-7 (inherently resistant to cisplatin). Furthermore, the resistance factor [defined as the ratio of IC_{50} values in resistant (A2780cisR) and cisplatin-sensitive parent cells (A2780)] was 1.0 and 0.77 for **1** and **2**, respectively, whereas it was markedly higher for cisplatin (6.5). This suggests that the mechanisms underlying the biological action of **1** and **2** is somewhat different from that of cisplatin allowing both compounds to overcome successfully the resistance mechanisms operating in the case of cisplatin.

Apart from the ability of compounds **1** and **2** to kill tumor cells resistant to clinically used cisplatin, the low cytotoxicity of **1** in noncancerous human primary skin fibroblasts demands special attention. The IC_{50} of **1** in noncancerous cells is more than one order of magnitude greater than that found for sensitive cancer cell line A2780. Thus, **1** shows selectivity for tumor cells relative to the nontumorigenic, normal, cells comparable to cisplatin, whereas the trans derivative **2** is somewhat less selective.

Cellular Accumulation. One of the key factors affecting the biological activity of metal-based drugs is the intracellular accumulation. To examine the ability of **1** and **2** to enter and accumulate in tumor cells, A2780, A2780cisR and MCF-7 cells were incubated with the platinum complexes for 5 and 24 h exposure times and the platinum content measured. The amount of platinum associated with the cells after only 10 s of treatment was also determined and assumed to represent the level of platinum adsorption on the cells surface. These values were subtracted from those found after 5 or 24 h exposure time. The platinum adsorption on the cell surface was approximately the same for **1** and **2** and very similar to that of cisplatin (not shown).

The intracellular accumulation of **1** was somewhat lower than that of cisplatin in cisplatin sensitive A2780 cells while it was very similar to that of cisplatin in resistant A2780cisR cells. Therefore the enhanced cytotoxic activity of **1** toward A2780cisR cells is not due to enhanced accumulation of the drug. Unlike A2780 and A2780cisR cells, the drug accumulation of **1** was greater than that of cisplatin in MCF-7 cells (2-3-fold increase), in agreement with the greater cytotocity of **1** towards this cell line.

Unlike **1**, the cellular uptake of **2** was markedly greater (3 - 9-fold) than that of cisplatin in all cell lines tested in this work (Table 3). This is in line with the lower polarity of trans compounds as compared to cis ones. A scale of hydrophobicity can be deduced from log P values for octanol/water partition. Log P values for cisplatin, **1** and **2** were -1.92,[29] -0.66 and 0.83, respectively, confirming that **2** is the most hydrophobic.

Table 3. Cellular Accumulation of 1, 2 and Cisplatin (at Equitoxic Concentrations) in A2780, A2780cisR or MCF-7 Tumor Cells[a]

	A2780		A2780cisR		MCF-7	
	5 h	24 h	5 h	24 h	5 h	24 h
cisplatin	89 ± 1	181 ± 23	44 ± 5	128 ± 2	46 ± 11	100 ± 15
1	60.1 ± 0.4	139 ± 29	40 ± 4	126 ± 34	94 ± 15	298 ± 64
2	269 ± 35	595 ± 24	243 ± 27	640 ± 28	446 ± 23	893 ± 21

[a] Intracellular accumulation of **1**, **2** and cisplatin at equitoxic concentrations (IC_{50}) in A2780, A2780cisR and MCF-7 cells after 5 h or 24 h. Each value shown in the Table 3 is in pmoles of platinum per 10^6 cells. Results are expressed as the mean ± SD for three independent experiments.

Notwithstanding the greater accumulation, the toxicity of **2** in these cancer cells is comparable to that of **1** (Table 2). For compounds **1** and **2**, the cellular uptake remains constant for sensitive and resistant ovarian cancer cells as does their cytotoxicity. In contrast, the cisplatin uptake decreases by 1.5-2-fold which results in an even greater decrease of cytotoxicity (6.5-fold). The greater toxicity of **1** and **2** toward MCF-7 cells, which are intrinsically resistant to cisplatin, correlates with a greater degree of drug uptake.

DNA Platination in Cells Exposed to Platinum Complexes. The cytostatic action of conventional platinum anticancer drugs is connected with their binding to nuclear DNA. The degree of DNA platination was determined by inductively coupled plasma mass spectrometry (ICP-MS) for the three cell lines after their exposure to **1**, **2** or cisplatin for 5 or 24 h (Table 4). The amount of platinum associated with DNA was determined (Table 5).

Table 4. Platinum Content of DNA Isolated from A2780, A2780cisR or MCF-7 Cells Treated with Equitoxic Doses of 1, 2 or Cisplatin[a]

	A2780		A2780cisR		MCF7	
	5 h	24 h	5 h	24 h	5 h	24 h
cisplatin	0.14 ± 0.03	0.34 ± 0.02	0.07 ± 0.02	0.10 ± 0.02	0.15 ± 0.01	0.24 ± 0.02
1	0.094 ± 0.005	0.39 ± 0.02	0.075 ± 0.002	0.31 ± 0.04	0.13 ± 0.02	0.43 ± 0.13
2	0.15 ± 0.02	0.51 ± 0.02	0.325 ± 0.002	0.94 ± 0.14	0.340 ± 0.003	0.82 ± 0.16

[a]Cells were exposed to tested compounds at equitoxic concentrations (IC_{50}) for 5 or 24 h. Each value shown in the Table 4 is in pmoles of Pt/μg of DNA. Results are expressed as the mean ± SD for three independent samples.

Table 5. Platinum Content of DNA Fraction Isolated from Cells Exposed to Equitoxic Doses of 1, 2 or Cisplatin Expressed as a Percentage of the Total Platinum Accumulated in the Cell[a]

	A2780		A2780cisR		MCF-7	
	5 h	24 h	5 h	24 h	5 h	24 h
cisplatin	1.1	1.3	1.1	0.6	2.3	1.7
1	1.1	1.9	1.3	1.7	1.0	1.0
2	0.4	0.6	0.8	1.0	0.5	0.6

[a]Cells were exposed to tested compounds at their equitoxic concentrations (IC_{50}) for 5 or 24 h.

After 5 h exposure time, the degree of DNA platination was comparable for **1** and cisplatin. At longer exposure time (24 h), platination was found similar for **1** and cisplatin

only in A2780 cells, while it was significantly greater for **1** than for cisplatin in resistant A2780cisR and MCF-7 cells (3.0- and 1.8-fold, respectively). Therefore, DNA platination appears to correlate with toxicity of **1** and cisplatin in the tumor cell lines tested in this work. This finding is in good agreement with the view that, similarly to cisplatin, DNA is the biological target for **1**.

Notably, for all cell lines and for all exposure times the amount of platinum bound to DNA was significantly greater (1.5 - 9-fold) in the case of **2** than in the case of **1**. However **2** had a cytotoxicity comparable to that of **1** (Table 3). Assuming that DNA is the pharmacological target also for Pt complexes with 1-Me-7-azaindol, these results suggest that **2** modifies DNA differently than **1** and that DNA adducts of **2** are inherently less effective than those of **1.**

From the data reported in Tables 3 and 4 it is possible to estimate the percentage of total platinum in the cells that binds to DNA. In most cases the percentage is lower for **2** than for **1** or cisplatin (Table 5).

DNA and Protein Binding in Cell-free Media. The experiments described above reveal that for **1** and **2** there is no direct correlation between the intracellular accumulation and the degree of DNA platination. To clarify this result, the DNA binding properties of **1** and **2** were studied in cell free media and compared to that of cisplatin. The platinum complexes were incubated with calf thymus (CT) DNA at r_i (r_i is defined as the molar ratio of free platinum complex to nucleotide phosphates at the onset of incubation with DNA) of 0.05 in $NaClO_4$ (10 mM) at 310 K in the dark. Aliquots were withdrawn at various time intervals, the free (unbound) platinum compound was removed by exhaustive dialysis, and the content of platinum and the concentration of DNA were determined by flameless atomic absorption spectrometry (FAAS) and absorption spectrophotometry, respectively. The results shown in Figure 6A indicate that after 24 h of incubation the platinum bound to DNA is 69 ± 4% and 95 ± 3 % for **1** and **2**, respectively (cisplatin binds to DNA quantitatively). These DNA binding experiments indicate that irreversible binding to DNA is somewhat slower for **1** than for **2** and cisplatin. Therefore, the lower portion of platinum bound to nuclear DNA, with respect to the total platinum taken up by the cell after 24 h, in the case of **2** cannot be a consequence of its lower DNA binding affinity. In other words, other factors, such as greater trapping of more lipophilic **2** into the cell membrane or greater reactivity of the trans compound for intracellular nucleophiles other than DNA (such as sulfur-containing species) may play a role.

The possibility that the intracellular pool of **1** and **2** that can reach and bind DNA can be reduced differently for these platinum complexes by interaction with intracellular nucleophiles was tested by investigating the interaction of **1** and **2** with human serum albumin (HSA). Therefore, **1** or **2** were incubated with HSA at molar ratio 1:1 in Tris.HCl (10 mM, pH 7.4) and in the presence of NaCl (8 mM) at 37 °C in the dark. Aliquots were withdrawn at various time intervals, the free (unbound) platinum compound was removed by exhaustive dialysis, and the content of platinum and the concentration of HSA were determined by FAAS and absorption spectrophotometry, respectively. The reaction of **2** with HSA was noticeably faster than that of **1 (**Figure 6B). Based on this outcome, we can hypothesize that a significantly higher fraction of **2** is trapped in the cytoplasm by reaction with intracellular proteins, peptides and/or other intracellular thiols and cannot access DNA. The higher reactivity of **2** towards the biomolecules present in the cytoplasm can thus be responsible for its lower efficiency to platinated DNA despite its higher accumulation in the cells.

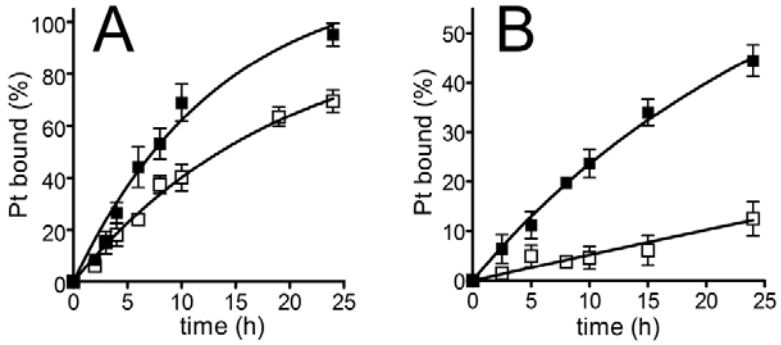

Figure 6. Reaction of **1** (open symbols) or **2** (closed symbols) with (A) double-helical CT DNA ($NaClO_4$ 0.01 M) and (B) human serum albumin in Tris.HCl (10 mM, pH 7.4) plus NaCl (8 mM) at 310 K as a function of time.

Transcription Mapping. Samples of DNA (the NdeI/HpaI fragment of pSP73KB plasmid) modified by **1** or **2** for analysis by transcription mapping were prepared in $NaClO_4$ (10 mM) at 310 K. After 24 h incubation with the complex, the DNA sample was precipitated with ethanol, then redissolved in the medium necessary for the transcription mapping analysis, while the r_b value (the number of molecules of platinum complex bound per nucleotide residue) in these samples was determined by platinum FAAS and by measurement of absorbance at 260 nm. By adopting this procedure, the transcription mapping analysis (described below) is performed in the absence of unbound (free) Pt complex.

Cutting of pSP73KB DNA by NdeI and HpaI restriction endonucleases yields a 212-base pairs (bp) fragment (a substantial part of its nucleotide sequence is shown in Figure 8B). This fragment contains a T7 RNA polymerase promotor. This DNA template was modified by **1** or **2** at $r_b = 0.01$ and its ability to terminate the *in vitro* RNA synthesis by T7 RNA polymerase at the level or in the proximity of platinum-DNA adducts was evaluated (Figure 7A). The major stop sites observed for **1** correspond to the sites for cisplatin, indicating similar DNA binding modes for both cis compounds. On the other hand, the pattern of stop sites obtained for compound **2** is similar to that found for transplatin (e.g. much less regular with respect to those of the cis compounds (Figure 7B).

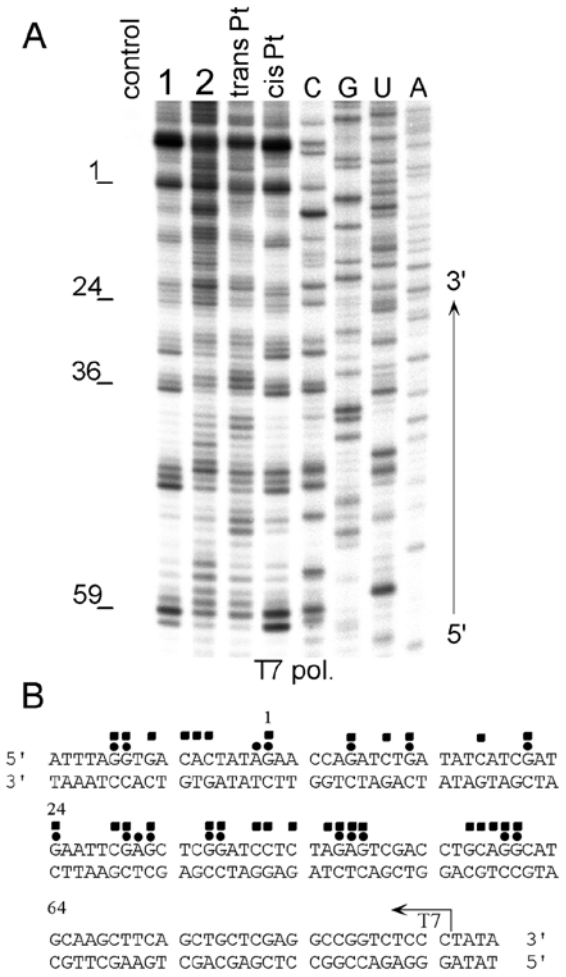

Figure 7. RNA synthesis by T7 RNA polymerase on the NdeI/HpaI fragment of pSP73KB plasmid modified by **1**, **2**, cisplatin or transplatin. A. Autoradiogram of 6% polyacrylamide/8 M urea sequencing gel. Lanes: control, nonplatinated template; 1, 2, transPt, cisPt, template modified by **1**, **2**, transplatin or cisplatin, respectively, at $r_b = 0.01$; C, G, U, and A chain terminated markers for nonplatinated template. B. Sequence of the NdeI/HpaI fragment of the pSP73KB plasmid. The arrow indicates the start of T7 RNA polymerase. Numbers correspond to nucleotide numbering in the sequence of the pSP73KB plasmid. Circles and squares indicate stop signals from panel A, lanes **1** and **2**, respectively.

Localization in Tumor Cells. A2780 cells were first exposed to **1** or **2** (30 μM) for 5 h and then visualized by confocal microscopy (Figure 8). After the treatment, cells were carefully washed with platinum-free medium so that no residual free platinum complex was present in the growing medium. No signal was yielded by the untreated cells (Figure 8C) or the cells treated with cisplatin (not shown), which suggests that the signal yielded by the cells treated with **1** or **2** comes only from the platinum complex containing 1M7AI ligand. The resulting images show that the subcellular localization of the light is largely non-nuclear. This is in good correlation with previously described data showing that only about 1% of total cell-associated platinum is localized on nuclear DNA. The signal appears to be localized mostly in cell organelles (for example in lysosomes or late endosomes) rather than on cytoplasmic membranes (Figures 8A,B). Data shown in Figures 8D,E are consistent with the thesis that the intracellular accumulation of **1** and **2** increases with the time of treatment and that the intracellular accumulation of **2** is significantly higher than that of **1**.

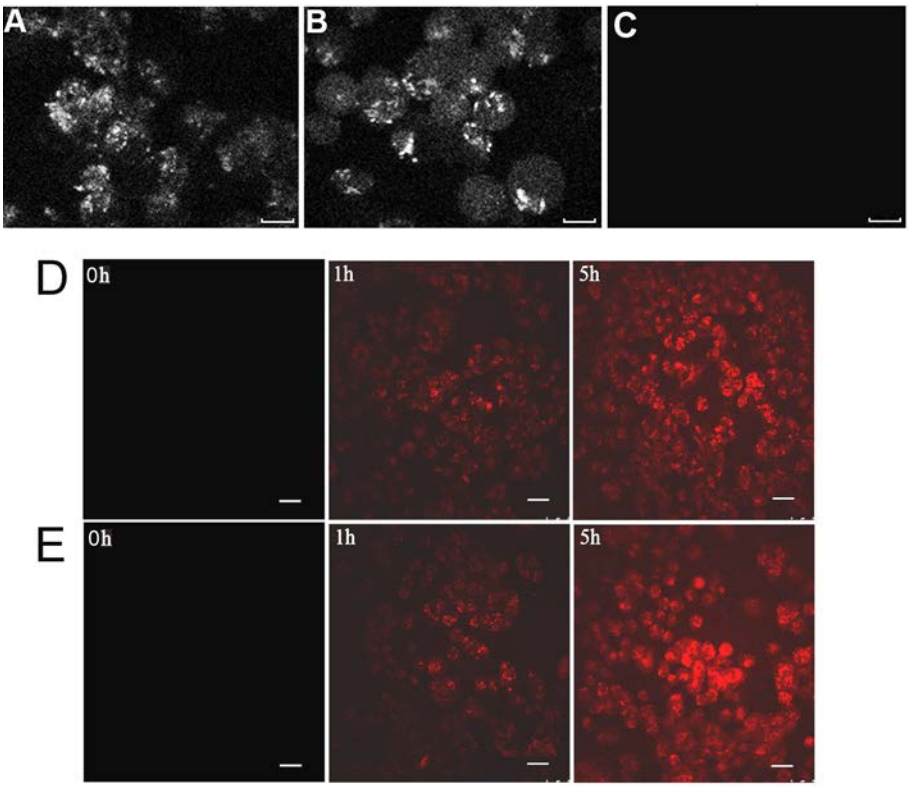

Figure 8. Top panels (A-C): Confocal microscope images of A2780 cells exposed to 30 µM **1** (A), **2** (B) for 5 h or which were untreated (C). Scale bars represent 10 µm.
Bottom panels (D,E): Confocal microscope images of A2780 cells treated with 30 µM of **1** (panels D) or **2** (panels E) for the time indicated in each panel. Scale bars represent 25 µm.

Cell Cycle Analysis. To further characterize the cytotoxic effect of **1** and **2**, an analysis of the cell cycle perturbations was performed in A2780 cells exposed to **1**, **2** or to reference compound cisplatin. Activation of cell cycle checkpoints is a general cellular response to cytotoxic agents. Previous studies have indicated that cisplatin and other platinum agents predominantly inhibit cell cycle progression at the S and/or G_2 phase.[30, 31] Cells were exposed to **1**, **2**, or cisplatin at their IC_{50} concentrations (Table 2) for 24 or 72 h. Significant differences in cell cycle modulation between **1** and **2** were observed already after 24 h of treatment and the differences became more pronounced as the treatment time increased (Figure 9).

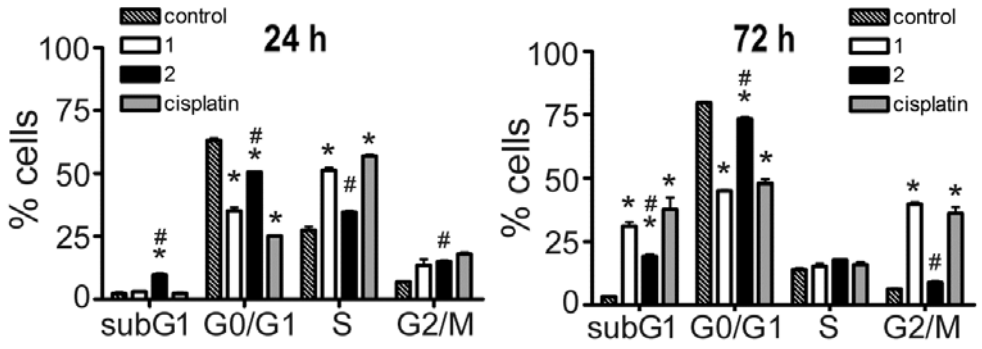

Figure 9. Effects of **1**, **2**, and cisplatin on cell cycle distribution. Untreated (control) A2780 cells or A2780 cells treated with equitoxic concentration of **1 (**4.2 µM), **2** (3.6 µM) or cisplatin (2.4 µM) for 24 h (left panel) or 72 h (right panel) were harvested, fixed, stained with propidium iodide, and assessed for cell cycle distribution by fluorescence-activated cell

sorting (FACS). The estimated percentages of A2780 cells in different phases of the cell cycle are indicated. The results are expressed as the mean ± the standard deviation (SD) of three independent experiments. The symbol (*) denotes a significant difference ($p < 0.05$) from the untreated control; (#) denotes a significant difference ($p < 0.05$) between **1** or **2** and cisplatin.

Exposure of A2780 cells to **1**, **2**, or cisplatin led to the appearance of a population in the sub-G_1 region (more evident after 72 h exposure), where apoptotic and necrotic cells are found. Therefore, the appearance of a sub-G_1 peak is consistent with the onset of internucleosomal DNA cleavage in late apoptosis.[31] Importantly, treatment with **2** affected the G_0/G_1 populations less than treatment with **1** or cisplatin. Unlike **2**, **1** and cisplatin caused significant accumulation of cells in the S-phase of the cell cycle at short exposure time (24 h) and cell cycle block in G_2-phase at long exposure time (72 h). These results are in agreement with data previously reported for cisplatin[31, 32] and highlight the similarity between cell cycle perturbations induced by **1** and cisplatin whereas **2**, having trans geometry, behaves differently.

Detection of Apoptosis and Necrosis. The levels of apoptosis and necrosis induced in A2780 cells by **1**, **2** or cisplatin at various concentrations over 24 and 72 h exposure time was quantified by the cell death detection ELISA colorimetric kit (ELISA = enzyme-linked immunosorbent assay). The assay is based on the quantitative "sandwich enzyme immunoassay" principle using mouse monoclonal antibodies directed against DNA and histones. This allows the specific determination of mono- and oligonucleosomes (histone-associated DNA fragments) in the cytoplasmic fraction of the cell lysates. The relative amounts of cytoplasmic histone-associated DNA fragments are measured after the induction of apoptosis or when these fragments are released from necrotic cells. Figure 10 shows DNA fragmentation induced by **1**, **2**, or cisplatin in A2780 cells.

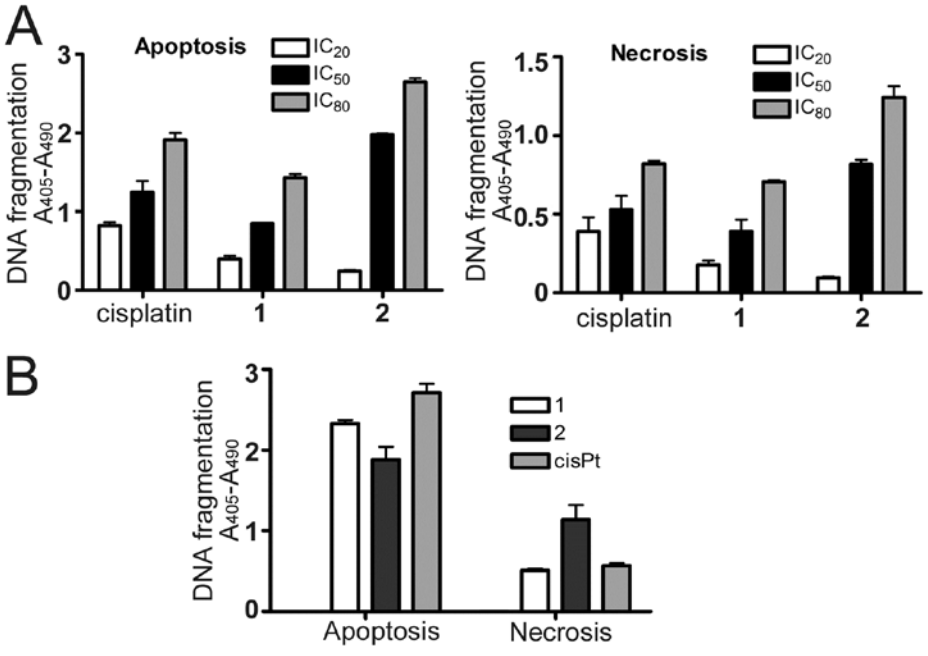

Figure 10. Effects of **1**, **2** and cisplatin on activation of the apoptotic and necrotic pathways in A2780 cells determined by DNA fragmentation ELISA assays. A. Cells treated for 24 h with **1**, **2** or cisplatin at the equitoxic concentrations indicated in the figure. Left panel, apoptosis; right panel, necrosis. B. Cells treated for 72 h with **1**, **2** or cisplatin at a concentration corresponding to the IC_{50} value (Table 2). The results are expressed as the mean of two

independent experiments with duplicate runs. The levels of DNA fragmentation found for control, untreated, cells were subtracted from each column.

The results demonstrate that treatment with all tested antitumor agents leads to concentration dependent apoptotic events in the A2780 cell line (Figure 10A). Importantly, **1** induces a lower level of DNA fragmentation, due to apoptosis, in comparison with cisplatin over the whole range of concentrations used. In contrast, **2** was less effective in inducing DNA fragmentation at low concentration (IC_{20}) compared to cisplatin, whereas at higher concentrations (corresponding to IC_{50} and IC_{80}) it was more effective than cisplatin. A similar ELISA assay was also used to detect the extent of necrosis induced by **1**, **2**, or cisplatin. Importantly, the level of necrosis was significantly lower compared to that of apoptosis triggered by **1**, **2**, or cisplatin (Figure 10B). At long treatment times, apoptosis predominates over necrosis, with **2** being less efficient in inducing apoptosis compared to the cis-compounds **1** and cisplatin (Figure 10B). The data are consistent with the results of flow cytometric measurements (Figure 9) where **2** was the most effective in inducing sub G_1 population of cells after 24 h of incubation, but the least efficient after 72 h.

To further explore this finding, we determined the cytotoxicities of **1**, **2** and cisplatin also after a short time of treatment. After 24 h of incubation of A2780 cells with the Pt(II) complexes, the IC_{50} values assessed by the MTT test [MTT = 3-(4,5-dimethylthiazol-2-yl)-2,5-diphenyltetrazolium bromide] were 47 ± 2, 9.4 ± 0.8, and 14.9 ± 0.9 μM for **1**, **2**, and cisplatin, respectively. These data also confirm that **2** is more effective in the early phases of the treatment, whereas the cytotoxic effect of **1** is manifested mostly after longer period of incubation (Figure 11).

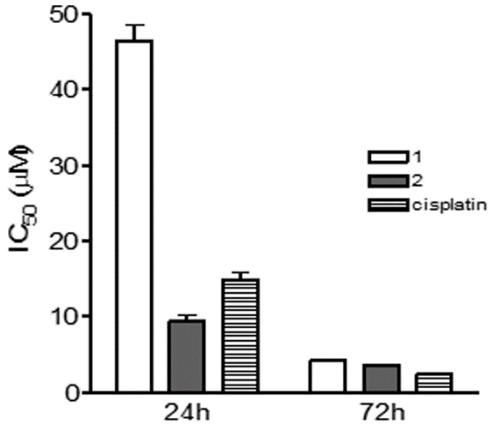

Figure 11. Comparison of IC_{50} values determined in A2780 cells for complexes **1**, **2** or cisplatin after 24 or 72 h treatment. The results are expressed as the mean ± SD of two independent experiments with quadruplicate runs.

CONCLUSIONS

The aim of this work was to exploit the effect of substitution of 1M7AI for one ammine in cisplatin (compound **1**). Cisplatin analogues in which one ammine has been replaced by a bulky N-donor ligand, such as 2-picoline in picoplatin, become less reactive towards physiologically relevant nucleophiles, which can improve their pharmacological properties. The 1M7AI ligand shares some similarities with 2-picoline and, in addition, can be used as a probe for confocal microscopy, thus allowing to monitor the faith of the drug in leaving cells. Methylation at position 1 of the 7-azaindole ring rules out the pH dependence of its optical

properties. For comparison, the corresponding trans compound (*trans*-[$PtCl_2(NH_3)$(1M7AI)], **2**) has also been synthesized and investigated.

The X-ray characterization of **1** has shown that, indeed, the 1M7AI ligand shields the metal core placing the methyl group at very short distance from platinum (Pt···H(C) distance of 2.78(9) Å). Moreover, the H-bond interactions between methyls and chlorido ligands (usually considered to be not particularly strong) within a pair of complex molecules results in an extraordinary short distance between the two methyls (C···C distance of 3.11(1) Å). Substitution of 1M7AI for NH_3 in the cis isomer increases significantly the activity of the drug towards cells with acquired (A2780cisR) or intrinsic resistance (MCF-7) to cisplatin. While for MCF-7 cells the increased toxicity could be a consequence of increased drug uptake, this is not the case for A2780cisR cells for which the cellular accumulation is similar for **1** and cisplatin. In the latter cell strain, however, in spite of similar uptake, the degree of DNA platination is greater for **1** than for cisplatin, which can explain its greater efficacy in full agreement with the view that, similarly to cisplatin, DNA is the biological target also for **1**.

This study also demonstrates that the trans geometry in Pt^{II}-dichlorido compounds can be also effectively activated by the replacement of one NH_3 ligand in transplatin by bulky 1M7AI (compound **2**) and, overall, **1** and **2** have similar activity towards the tumor cells tested. This investigation has nicely shown how two factors contribute significantly to the antitumor activity of trans compounds: the greater cellular uptake (mainly dependent upon their lower polarity) and the greater reactivity towards DNA (N-donor ligands with low trans-activation ability in cis position to the DNA-binding site). In contrast, detrimental for their antitumoral activity is the greater reactivity of trans compounds towards physiologically relevant nucleophiles.

Confocal microscopy experiments confirm the data on cellular accumulation and extent of DNA platination. Finally, cell cycle analysis and cell death detection by ELISA assays indicate that at long treatment time apoptosis predominates over necrosis with the trans compound being less efficient in inducing apoptosis compared to the cis compounds. This investigation represents a further step in unraveling differences and analogies in the mechanism of action of strictly related cis and trans complexes of mononuclear platinum. In addition, the activity of the new compounds is such to merit further investigation.

EXPERIMENTAL SECTION

Commercial reagent grade chemicals and solvents were used as received without further purification. Cisplatin, N,N′-dimethylformamide (DMF), human serum albumin (HSA), and propidium iodide were from Sigma-Aldrich (Prague, Czech Republic). 1-Methyl-7-azaindole was from Ark Pharm, Inc. (Libertyville, USA). CT DNA (42% G+C, mean molecular mass ca. $2x10^7$) was prepared and characterized as described previously.[33, 34] Plasmid pSP73KB (2455 bp) was isolated according to standard procedures. Restriction endonucleases were purchased from New England Biolabs. Acrylamide and bis(acrylamide) were obtained from Merck KgaA (Darmstadt, Germany). MTT was from Calbiochem (Darmstadt, Germany). [α-^{32}P]CTP was obtained from MP Biomedicals, LLC (Irvine, CA). RNase A was from Qiagen (USA). DNazol (genomic DNA isolation reagent) was obtained from MRC (Cincinnati, OH). RPMI 1640 medium, fetal bovine serum (FBS), trypsin/EDTA, and Dulbecco's modified Eagle's medium (DMEM) were from PAA (Pasching, Austria). Penicilin, gentamycin and streptomycin was from Serva (Heidelberg, Germany). Riboprobe Gemini System II for transcription mapping containing T7 RNA polymerase was purchased from Promega

(Madison, WI). Cell death detection ELISA plus kit was from Roche Molecular Biochemicals (Mannheim, Germany).

Synthesis. K[$PtCl_3(NH_3)$] and cis-[$PtI_2(NH_3)_2$] were prepared according to already reported procedures.[13, 35] The elemental analysis and the spectroscopic features were fully consistent with the data reported in the literature.

*Cis-[$PtCl_2(NH_3)$(1M7AI)] (**1**).* K[$PtCl_3(NH_3)$] (0.26 g, 0.71 mmol) was suspended in CH_3OH (40 mL) and treated with a slight excess of 1M7AI (0.115 g, 0.84 mmol). The mixture was kept under stirring at room temperature for 4 days and then the suspension was filtered through Celite and the pale yellow solution was evaporated to dryness under reduced pressure. The solid residue was triturated with CH_2Cl_2 (8 mL) in order to remove the excess of ligand. The obtained suspension was filtered off and the resulting yellow solid was dried under vacuum, washed with warm water (328 K) to remove KCl, dried again under vacuum and analyzed by TLC using dichloromethane/acetone 1:1 as eluent. The chromatogram showed one single spot, corresponding to **1**, in addition to some non-eluting side products. Therefore, the raw material was subjected to silica gel chromatography, using dichloromethane/acetone 1:1 as eluent. Were obtained 0.14 g (0.34 mmol, 48% yield) of **1**. Anal. Calculated for *cis*-[$PtCl_2(NH_3)$(1M7AI)]·CH_3OH ($C_8H_{11}N_3Cl_2Pt·CH_3OH$): C, 24.16; H, 3.38; N, 9.40%. Found: C, 23.83; H, 2.99; N, 9.65%. ^{1}H-NMR (acetone-d_6) δ: 8.89 (m, 1 H, H_6), 8.06 (m, 1 H, H_4), 7.55 (m, 1 H, H_2), 7.10 (m, 1 H, H_5), 6.63 (d, 1 H, H_3), 5.24 (s, 3 H, CH_3), 4.10 (b, 3 H, NH_3) ppm. ^{195}Pt-NMR (acetone-d_6) δ: −1,970 ppm. ESI-MS: calculated for $[C_8H_{11}N_3Cl_2PtNa]^+$ 437.98. *Found: m/z* (% relative to the base peak) 437.9 (100), [M + Na]$^+$.

*Trans-[$PtCl_2(NH_3)$(1M7AI)] (**2**).* Compound **2** was prepared by a two-step process which involved the preparation of the intermediate species *trans*-[$PtI_2(NH_3)$(1M7AI)]. *Trans*-[$PtI_2(NH_3)$(1M7AI)] was prepared from *cis*-[$PtI_2(NH_3)_2$] and 1M7AI. *cis*-[$PtI_2(NH_3)_2$] (1.01 g, 2.09 mmol) was reacted with $AgNO_3$ (0.71 g, 4.19 mmol) in H_2O (50 mL) and kept at 328 K in the dark for 20 min. The AgI precipitate was separated by filtration and the clear solution treated with a twofold excess of 1M7AI (0.55 g, 4.19 mmol). The mixture was heated at 343 K for 3 h; then the suspension was filtered through Celite and the yellow mother solution containing *cis*-$[Pt(NH_3)_2(1M7AI)_2]^{2+}$ was treated with an aqueous solution of KI (1.74 g, 1.05 mmol), added dropwise over a period of 5 min. The solution was stirred at 343 K for 2 h, meanwhile a brown precipitate formed. The brown solid was collected by filtration of the mother liquor and left to dry under vacuum. The solid residue was triturated with a mixture of acetone/dichloromethane (1:1, v/v; 100 mL), the solution was separated by filtration, the solvent was evaporated under reduced pressure, and the solid residue analyzed by TLC using dichloromethane/acetone 9:1 as eluent. The chromatogram showed two spots, corresponding (in order of increasing R_f) to *trans*-[$PtI_2(NH_3)$(1M7AI)] and *trans*-[PtI_2(1M7AI)$_2$]. Therefore, the raw materials was subjected to silica gel chromatography, using dichloromethane/acetone 9:1 as eluent. Were obtained 0.250 g (0.42 mmol, 20% yield) of *trans*-[$PtI_2(NH_3)$(1M7AI)]. Anal. Calculated for *trans*-[$PtI_2(NH_3)$(1M7AI)] ($C_8H_{11}N_3I_2Pt$): C, 16.05; H, 1.84; N, 7.02%. Found: C, 16.65; H, 1.91; N, 6.89%. ^{1}H-NMR (acetone-d_6,) δ: 8.72 (m, 1 H, H_6), 7.97 (m, 1 H, H_4), 7.50 (m, 1 H, H_2), 7.03 (m, 1 H, H_5), 6.59 (d, 1 H, H_3), 5.17 (s, 3 H, CH_3), 3.88 (b, 3 H, NH_3) ppm. ^{195}Pt-NMR (acetone-d_6) δ: −3,240 ppm. *ESI-MS:* calculated for $[C_8H_{11}N_3I_2PtNa]^+$ 621.07. *Found: m/z* (% relative to the base peak) 621.05(100), [M + Na]$^+$.

The dichlorido complex **2** was prepared from *trans*-[$PtI_2(NH_3)$(1M7AI)] (0.11 g, 0.18 mmol) dissolved in H_2O (50 mL) and treated with $AgNO_3$ (0.060 g, 0.37 mmol). After 3 h stirring at 323 K and in the dark, the solution was filtered (to remove the AgI precipitate), treated with an excess of KCl (0.13 g, 1.8 mmol) and kept at 328 K for 1 h, during which time a brown solid precipitated from the solution. The suspension was concentrated to a minimum

volume under reduced pressure, while keeping the reaction vessel at 328 K, and then cooled to 277 K in order to promote further precipitation of the desired product. The solid residue was transferred on a glass filter, washed with a minimum amount of cold water, dried under vacuum and analyzed by TLC using dichloromethane/acetone 9:1 as eluent. The chromatogram showed one single spot, corresponding to **2**, in addition to some non-eluting side products. Therefore, the raw material was subjected to silica gel chromatography, using dichloromethane/acetone 9:1 as eluent. Were obtained 0.037 g (0.089 mmol, 50% yield) of **2**. Anal. Calculated for *trans*-[$PtCl_2(NH_3)(1M7AI)$]·¼CH_3COCH_3 ($C_8H_{11}N_3Cl_2Pt$·¼CH_3COCH_3): C, 24.44; H, 2.91; N, 9.78%. Found*:* C, 24.70; H, 2.92; N, 10.09%. ^{1}H-NMR (acetone-d_6) δ: 8.71 (m, 1 H, H_6), 8.03 (m, 1 H, H_4), 7.51 (m, 1 H, H_2), 7.09 (m, 1 H, H_5), 6.61 (d, 1 H, H_3), 5.17 (s, 3 H, CH_3), 3.85 (b, 3 H, NH_3) ppm. ^{195}Pt-NMR (acetone-d_6) δ: −1,967 ppm. *ESI-MS:* calculated for [$C_8H_{11}N_3Cl_2PtNa$] 438.18. *Found: m/z* (% relative to the base peak) 437.9(100), $[M + Na]^+$.

X-ray crystallography. Crystals suitable for X-ray investigation were obtained from water/acetone (1:2 ratio). Reflections were collected with Mo-*K*α radiation by using a Bruker AXS X8 APEX CCD System. All reflections were indexed, integrated, and corrected for Lorentz, polarization, and absorption effects using the program SADABS [Sheldrick G. M., SADABS University of Göttingen Germany (1996)]. Data collection, data reduction, and unit cell refinement were carried out with the SAINT-IRIX package [Bruker: SAINT-IRIX BrukeRAXSInc Madison Wisconsin USA (2003)].

The model was refined by full-matrix least-square methods. All non-hydrogen atoms were refined anisotropically. The H atoms of the amino and methyl groups were found in a difference Fourier map and were refined with Uiso(H) = 1.5 Ueq(parent). Hydrogen atoms of aromatic rings were placed at calculated positions and refined given isotropic parameters equivalent to 1.2 times those of the atom to which they are attached. All calculations and molecular graphics were carried out using SIR2004,[36] SHELXL97,[37] PARST97,[38, 39] WinGX,[40] and ORTEP-3 for Windows packages.[41] Details of the crystal data are listed in Table 2.

Table 2. Crystal Data and Structure Refinement for *cis*-[$PtCl_2(NH_3)(1M7AI)$] (1).

Empirical formula	$C_8H_{11}Cl_2N_3Pt$
Formula weight	415.19
Crystal system	orthorhombic
Space group	*Pbca*
Unit cell dimensions (Å)	*a* = 10.1183(2)
	b = 10.4734(2)
	c = 21.2984(4)
Volume (Å^3)	2257.06(8)
Z	8
dimension (mm^3)	1.000 x 0.225 x 0140
Density (Mg/m^3)	2.444
Absorption coefficient (mm^{-1})	12.871
F(000)	1536
Theta range for data collection (°)	1.91 to 30.51
Index ranges	-14≤h≤14
	-14≤k≤14
	-30≤l≤30
Reflections collected	49459

Independent reflections	3447 [R(int) = 0.0280]
Data / restraints / parameters	3447 / 0 / 145
Goodness-of-fit on F^2	1.156
Final R indices [I>2sigma(I)]	R1 = 0.0301, wR2 = 0.0655
R indices (all data)	R1 = 0.0478, wR2 = 0.0760
Largest diff. peak and hole (e $Å^{-3}$)	2.385 and -1.064

Crystallographic data (without structure factors) have been deposited with the Cambridge Crystallographic Data Centre as supplementary publication no. CCDC 1024413. Copies of the data can be obtained free of charge from the CCDC (12 Union Road, Cambridge CB2 1EZ, UK; tel: (+44) 1223-336-408; fax: (+44) 1223-336-003; e-mail: deposit@ccdc.cam.ac.uk; website http://www.ccdc.cam.ac.uk/data_request/).

Cell Lines and Culture. The human ovarian carcinoma A2780 (parent cisplatin-sensitive), A2780cisR (cisplatin resistant variant of A2780) and human breast adenocarcinoma MCF-7 (cisplatin in-born resistance) cell lines were supplied by Professor B. Keppler, University of Vienna (Austria). The A2780 and A2780cisR cells were grown in RPMI 1640 medium supplemented with streptomycin (100 μg mL^{-1}), penicilin (100 U mL^{-1}) and heat inactivated FBS (10%). The acquired resistance of A2780cisR cells was maintained by supplementing the medium with cisplatin (1 μM) every second subculture. The MCF-7 cells were grown in DMEM supplemented with streptomycin (100 μg mL^{-1}), penicilin (100 U mL^{-1}) and heat inactivated FBS (10%). The cells were cultured in a humidified incubator at 310 K in an atmosphere of 5% CO_2 and subcultured 2−3 times per week with an appropriate plating density. Human skin fibroblasts (primary cell culture) was a kind gift from Professor T. Adam, Laboratory of Inherited Metabolic Disorders, Department of Clinical Chemistry, Palacky University and Hospital, Olomouc, Czech Republic. These cells were grown in DMEM supplemented with streptomycin (100 μg mL^{-1}), penicilin (100 U mL^{-1}) and 10% heat inactivated FBS.

***In Vitro* Growth Inhibition Assay.** Influence of platinum complexes on cell viability was tested using the colorimetric MTT assay. Cells were seeded on 96-well tissue culture plates at a density of 10^4 cells/well in 100 μL of growth medium and incubated at 310 K in a humidified 5% CO_2 atmosphere for 16 h (overnight). After the incubation period the cells were treated with the compounds under investigations and kept in the incubator for additional 72 h. The stock solutions of platinum compounds were always freshly prepared in DMF before use. The final concentration of DMF in cell culture medium did not exceed 0.1% (v/v), which was shown not to affect cell growth. The final concentrations of tested compounds were in the range of 0 to 50 μM in a volume of 200 μL/well. Subsequently, 10 μL of MTT solution (5 mg mL^{-1}) was added to each well, and plates were incubated for 4 h. At the end of the incubation time the medium was removed and the formazan product was dissolved in 100 μL of DMSO per well. Cell viability was evaluated by measuring the absorbance at 570 nm (reference wavelength at 630 nm) using an Absorbance Reader Sunrise Tecan Schoeller. IC_{50} values were calculated from curves constructed by plotting cell survival (%) versus drug concentration (μM). All experiments were done in triplicate. The reading values were converted to the percentage of control (% cell survival). Cytotoxic effects were expressed as IC_{50}.

Cellular Accumulation. Cellular uptake of **1**, **2**, and cisplatin was measured in A2780, A2780cisR and MCF-7 cell lines. The cells were seeded on 100 mm tissue culture dishes ($3x10^6$ cells/dish in 10 mL of growth medium). After 48 h of incubation, the cells were treated with tested compounds (at their IC_{50} values) for 10 s, 5 or 24 h (the concentrations were verified by measuring the platinum content in the growing medium by FAAS). The attached cells were harvested by trypsinization and the cell pellets washed twice with cold PBS

(phosphate buffered saline) (277 K). The pellets were digested by using microwave acid (HCl) digestion system (MARS5, CEM) to give a fully homogenized solution. Final platinum content in the samples was determined by ICP-MS. The results of cellular platinum uptake were corrected for adsorption effects.[42]

Determination of Partition Coefficients of Platinum Complexes. Partition coefficients of **1** and **2** were determined in an octanol/saline system. Briefly, saline solution (100 mM NaCl) and n-octanol were pre-saturated with n-octanol and saline, respectively; then **1** or **2** (10^{-3} g, 2.41 x 10^{-3} mmol) was dissolved in saline (3 mL and 10 mL for **1** and **2**, respectively) at 310 K and the complex concentration was determined by FAAS. Equal volumes of the drug solution and n-octanol were placed in a glass tube and the mixture shaken mechanically for 1 h at 310 K. Then the mixture was centrifuged (1500 rpm, 5 min) and the bottom aqueous layer was removed and subjected to platinum analysis by FAAS. The complex concentration in the n-octanol phase was calculated by the difference between the complex concentration in saline before and after n-octanol extraction. Each value reported in the text represents a mean of triplicate determination; differences between the mean and individual values were <5%.

DNA Platination in Cells Exposed to Platinum Complexes. A2780, A2780cisR or MCF-7 cells grown to near confluence were treated with **1**, **2** or cisplatin at IC_{50} values and incubated for 5 or 24 h. After incubation, the cells were trypsinized and washed twice in ice-cold PBS. Cells were lysed in DNAzol (DNAzol genomic DNA isolation reagent) supplemented with RNase A (100 μg mL^{-1}). The genomic DNA was precipitated from the lysate with ethanol, dried, and resuspended in water. The DNA content in each sample was determined by UV spectrophotometry. To avoid the effect of high DNA concentration on detection of platinum in the samples, the DNA samples were digested in the presence of hydrochloric acid using a high pressure microwave mineralization system. Experiments were performed in triplicate, and the values are the means ± SD.

Platination Reactions in Cell-free Media. CT or plasmid DNAs were incubated with the platinum complexes in $NaClO_4$ (10 mM) at 310 K in the dark. After 24 h, the samples were exhaustively dialyzed against the medium required for subsequent biochemical or biophysical analysis. An aliquot of these samples was used to determine r_b values by FAAS. Similarly, HSA was incubated with the platinum complexes (molar ratio of 1:1) in Tris.HCl (10 mM, pH 7.4) plus NaCl (8 mM) at 310 K in the dark. Aliquots were withdrawn at various time intervals, quickly cooled to 193 K and exhaustively dialyzed against water. The platinum content in these samples was determined by FAAS, while the concentration of HSA was determined by absorption spectrophotometry.

DNA Transcription by RNA Polymerase *In Vitro*. Transcription of the pSP73KB DNA with T7 RNA polymerase and electrophoretic analysis of the transcripts were performed as previously described.[43] The concentration of DNA used in this assay was $3.9x10^{-5}$ M (relative to the monomeric nucleotide content).

Cell Cycle Analysis. A2780 cells were seeded on 60 mm tissue culture dishes at a density of $2x10^6$ cells/dish in 6 mL of growth medium and incubated at 310 K in a humidified 5% CO_2 atmosphere overnight. After incubation, the cells were treated with the compounds at IC_{50} values and stored at culture conditions. After 24 h, floating cells were collected, and attached cells were harvested by trypsinization (trypsin/EDTA in PBS). Total cells (floating + attached) were washed twice in PBS (277 K), fixed in 70% ethanol, and stored at 253 K. Cell pellets were subsequently rinsed with PBS buffer and the sediment was stained with solution of propidium iodide (50 μg mL^{-1}) supplemented by RNase A (10 μg mL^{-1}) for 30 min at room temperature in the dark. The DNA content of the cells was analyzed using flow cytometry (Cell lab quanta TM SC-MPL, Beckman Coulter). The percentages of cells in individual cell cycle phases were analyzed using Multicycle AV for Windows (Phoenix Flow Systems, USA).

Detection of Apoptosis and Necrosis. The cell death detection ELISA plus kit (Roche Molecular Biochemicals, Mannheim, Germany) was used as an indicator of apoptosis and necrosis.[44] In this assay, internucleosomal DNA fragmentation was quantitatively assayed by antibody-mediated capture and detection of cytoplasmic mononucleosome- and oligonucleosome-associated histone-DNA complexes. The treated A2780 cells were centrifuged (200 g, 10 min, room temperature), 20 μL of the supernatant (necrotic fraction) was used in the ELISA for detection of necrosis. A2780 cells were resuspended in 200 μL of the lysis buffer supplied by the manufacturer and incubated for 30 min at room temperature. After pelleting of the nuclei (200 g, 10 min, room temperature), 20 μL of the supernatant (cytoplasmic fraction) was used in the ELISA for detection of apoptosis following the manufacturer's standard protocol. Following incubation with peroxidase substrate for 20 min, absorbance was determined at 405 nm (reference wavelength was 490 nm) with a microplate reader (absorbance reader Tecan INFINITE M200, Schoeller). Signals from wells containing the substrate only were subtracted as background. Other details of this assay and data analysis were performed according to the manufacturer's instructions.

Confocal Microscopy. A2780 cells were seeded on glass bottom dishes (P50G-0-30-F, MatTek Co., Ashland, USA) at the density $1.5x10^6$ cells per dish and incubated at 310 K in a humidified 5% CO_2 atmosphere overnight. The cells were than treated with **1** or **2** (30 μM concentration) for 1 or 5 h. After this period, the cells were washed twice with PBS and supplemented with fresh medium (without compound). The distribution of tested compounds in tumor cells was analyzed by confocal microscopy. Samples were visualized with confocal microscope Leica TSC SP-5 X, sequentially scanned with the objective HCX PL APO lambda blue 63.0x1.20 water UV, corrected with an appropriate beam path. Resolution of captured images was 512·512 pix scanned with 100 Hz frequency. Samples were illuminated with UV laser at 355 nm and the light returning from the samples was detected with highly sensitive hybrid detectors at wavelengths 710-760 nm. Signal intensity associated with single cells was analyzed in the center of captured image (256·256pix) to omit potential objective aberrations. The experiment was repeated twice with three replicates of each sample. Settings of the imaging software (laser strength and gain) were kept constant within each experiment to allow for comparison of the light intensities of samples.

Physical Measurements. NMR spectra were collected at 295 K on a Bruker AVANCE DPX 300 MHz nominal ^1H Larmor frequency. ^1H chemical shifts were referenced to TMS by using the residual protic peak of the solvent (acetone-d_6, or D_2O) as internal reference. One-dimensional ^{195}Pt spectra were acquired using ^1H decoupling sequences. ^{195}Pt chemical shifts were referenced to K_2PtCl_4 (1 M in water, $\delta = -1{,}614$ ppm). Elemental analyses were carried out on a CHN Eurovector EA 3011 equipment. ESI-MS analyses were performed on an Agilent 1100 series LC-MSD Trap system VL. Absorption spectra were measured with a Beckmann DU-7400 spectrophotometer. FAAS measurements were carried out with a Varian AA240Z Zeeman atomic absorption spectrometer equipped with a GTA 120 graphite tube atomizer. The analysis with the aid of ICP-MS was performed using Agilent 7500 (Agilent, Japan). The gels were dried and visualized using a FUJIFILM BAS 2500 bioimaging analyzer.

Acknowledgements
The authors acknowledge support from the National Program of Sustainability I (LO1204), Operational Program Education for Competitiveness - European Social Fund (CZ 1.07/2.3.00/20.0057) of the Ministry of Education, Youth and Sports of the Czech Republic, the University of Bari “Aldo Moro”, the Consorzio Interuniversitario di Ricerca in Chimica dei Metalli nei Sistemi Biologici (CIRCMSB), the Italian Ministero dell’Università e della Ricerca (PON 01078 and FIRB RINAME RBAP114AMK). This research was also

supported by Palacky University in Olomouc (IGAPrF2014029). J.K.'s research was supported by the Ministry of Education, Youth and Sports of the Czech Republic (Grant LD14019). The authors acknowledge that their participation in the EU COST Action CM1105 enabled them to exchange regularly the most recent ideas in the field of metallodrugs with several European colleagues.

ABBREVIATIONS USED

1, *cis*-[$PtCl_2(NH_3)$(1M-7AI)]; **2**, *trans*-[$PtCl_2(NH_3)$(1M7AI)]; 1M7AI, 1-methyl-7-azaindole; bp, base pair; cisplatin, *cis*-diamminedichloridoplatinum(II); CT, calf thymus; DMEM, Dulbecco's modified Eagle's medium; DMF, N,N-dimethylformamide; ELISA, enzyme-linked immunosorbent assay; FAAS, flameless atomic absorption spectrometry; FBS, fetal bovine serum; HSA, human serum albumin; IC_{50}, concentration of compound which causes death in 50 % of cells; ICP-MS, inductively coupled plasma mass spectrometry; MTT, 3-(4,5-dimethylthiazol-2-yl)-2,5-diphenyltetrazolium bromide; PBS, phosphate saline buffer; picoplatin, *cis*-amminedichlorido(2-methylpyridine)platinum(II); r_b, the number of molecules of platinum complex bound per nucleotide residue; r_i, the molar ratio of free platinum complex to nucleotide phosphates at the onset of incubation with DNA; transplatin, *trans*-diamminedichloridoplatinum(II)

REFERENCES

(1) Page, J. D.; Husain, I.; Sancar, A.; Chaney, S. G. Effect of the diaminocyclohexane carrier ligand on platinum adduct formation, repair, and lethality. *Biochemistry* **1990,** *29*, 1016-1024.

(2) Kasparkova, J.; Marini, V.; Najajreh, Y.; Gibson, D.; Brabec, V. DNA binding mode of the cis and trans geometries of new antitumor nonclassical platinum complexes containing piperidine, piperazine or 4-picoline ligand in cell-free media. Relations to their activity in cancer cell lines. *Biochemistry* **2003,** *42*, 6321-6332.

(3) Kasparkova, J.; Novakova, O.; Najajreh, Y.; Gibson, D.; Perez, J.-M.; Brabec, V. Effects of a piperidine ligand on the mechanism of action of antitumor cisplatin. *Chem. Res. Toxicol.* **2003,** *16*, 1424-1432.

(4) Wurtenberger, I.; Angermaier, B.; Kircher, B.; Gust, R. Synthesis and in vitro pharmacological behavior of platinum(II) complexes containing 1,2-diamino-1-(4-fluorophenyl)-2-alkanol ligands. *J. Med. Chem.* **2013,** *56*, 7951-7964.

(5) Starha, P.; Travnicek, Z.; Popa, A.; Popa, I.; Muchova, T.; Brabec, V. How to modify 7-azaindole to form cytotoxic Pt(II) complexes: Highly in vitro anticancer effective cisplatin derivatives involving halogeno-substituted 7-azaindole. *J. Inorg. Biochem.* **2012,** *115*, 57-63.

(6) Muchova, T.; Pracharova, J.; Starha, P.; Olivova, R.; Vrana, O.; Benesova, B.; Kasparkova, J.; Travnicek, Z.; Brabec, V. Insight into the toxic effects of cis-dichloridoplatinum(II) complexes containing 7-azaindole halogeno derivatives in tumor cells. *J. Biol. Inorg. Chem.* **2013,** *18*, 579-589.

(7) Molenaar, C.; Teuben, J. M.; Heetebrij, R. J.; Tanke, H. J.; Reedijk, J. New insights in the cellular processing of platinum antitumor compounds, using fluorophore-labeled platinum complexes and digital fluorescence microscopy. *J. Biol. Inorg. Chem.* **2000,** *5*, 655-665.

(8) Safaei, R.; Katano, K.; Larson, B. J.; Samimi, G.; Holzer, A. K.; Naerdemann, W.; Tomioka, M.; Goodman, M.; Howell, S. B. Intracellular localization and trafficking of fluorescein-labeled cisplatin in human ovarian carcinoma cells. *Clin. Cancer Res.* **2005,** *11*, 756-767.

(9) Wu, S. D.; Wang, X. Y.; Zhu, C. C.; Song, Y. J.; Wang, J.; Li, Y. Z.; Guo, Z. J. Monofunctional platinum complexes containing a 4-nitrobenzo-2-oxa-1,3-diazole fluorophore: Distribution in tumour cells. *Dalton Trans.* **2011,** *40*, 10376-10382.
(10) Kelland, L. The resurgence of platinum-based cancer chemotherapy. *Nature Rev. Cancer* **2007,** *7*, 573-584.
(11) Hamilton, G.; Olszewski, U. Picoplatin pharmacokinetics and chemotherapy of non-small cell lung cancer. *Expert Opin. Drug Metabol. Toxicol.* **2013,** *9*, 1381-1390.
(12) New, E. J.; Roche, C.; Madawala, R.; Zhang, J. Z.; Hambley, T. W. Fluorescent analogues of quinoline reveal amine ligand loss from cis and trans platinum(II) complexes in cancer cells. *J. Inorg. Biochem.* **2009,** *103*, 1120-1125.
(13) Margiotta, N.; Denora, N.; Ostuni, R.; Laquintana, V.; Anderson, A.; Johnson, S. W.; Trapani, G.; Natile, G. Platinum(II) complexes with bioactive carrier ligands having high affinity for the translocator protein. *J. Med. Chem.* **2010,** *53*, 5144-5154.
(14) Rochon, F. D.; Buculei, V. Multinuclear NMR study and crystal structures of complexes of the types cis- and trans-Pt(amine)$_2$I$_2$. *Inorg. Chim. Acta* **2004,** *357*, 2218-2230.
(15) Pregosin, P. S. Platinum-195 nuclear magnetic resonance. *Coord. Chem. Rev.* **1982,** *44*, 247-291.
(16) Natile, G.; Maresca, L.; Cattalini, L. The $^4J_{PtH}$ coupling constant in platinum–hydrazone complexes: relative magnitude of the coupling constant between an alkyl group and a metal atom which are mutually cis- and trans- with respect to the azomethine double bond *J. Chem. Soc., Chem. Commun.* **1976**, 24-25.
(17) Boccarelli, A.; Intini, F. P.; Sasanelli, R.; Sivo, M. F.; Coluccia, M.; Natile, G. Synthesis and in vitro antitumor activity of platinum acetonimine complexes. *J. Med. Chem.* **2006,** *49*, 829-837.
(18) Maresca, L.; Natile, G.; Gasparrini, F.; Cattalini, L. Complexes of hydrazones with dichloro(η-ethylene)platinum(II): stereo-chemical and conformational analysis of the co-ordinated ligand *J. Chem. Soc., Dalton Trans.* **1976**, 1090-1093.
(19) Ludwig, T.; Riethmuller, C.; ller, C.; Gekle, M.; Schwerdt, G.; Oberleithner, H. Nephrotoxicity of platinum complexes is related to basolateral organic cation transport. *Kidney Int.* **2004,** *66*, 196-202.
(20) Michelin, R. A.; Bertani, R.; Mozzon, M.; Sassi, A.; Benetollo, F.; Bombieri, G.; Pombeiro, A. J. L. Cis addition of dimethylamine to the coordinated nitriles of cis- and trans-PtCl$_2$(NCMe)$_2$. X-ray structure of the amidine complex cis-PtCl$_2${E-N(H)=C(NMe$_2$)Me}$_2$.CH$_2$Cl$_2$. *Inorg. Chem. Commun.* **2001,** *4*, 275-280.
(21) Raudaschl, G.; Lippert, B.; Hoeschele, J. D.; Howard-Lock, H. E.; Lock, C. J. L.; Pilon, P. Adduct formation of cis-(NH$_3$)$_2$PtX$_2$ (X = Cl$^-$, I$^-$) with formamides and the crystal structures of cis-(NH$_3$)$_2$PtCl$_2$·(CH$_3$)$_2$NCHO. Application for the purification of the antitumor agent cisplatin. *Inorg. Chim. Acta, Bioinorg.Chem.* **1985,** *106*, 141-150.
(22) Ruiz, J.; Rodriguez, V.; de Haro, C.; Espinosa, A.; Perez, J.; Janiak, C. New 7-azaindole palladium and platinum complexes: crystal structures and theoretical calculations. In vitro anticancer activity of the platinum compounds. *Dalton Trans.* **2010,** *39*, 3290-3301.
(23) Brookhart, M.; Green, M. L. H.; Parkin, G. Agostic interactions in transition metal compounds. *Proc. Natl. Acad. Sci. USA* **2007,** *104*, 6908-6914.
(24) Bondi, A. van der Waals volumes and radii. *J. Phys. Chem.* **1964,** *68*, 441-451.
(25) Bruno, I. J.; Cole, J. C.; Lommerse, J. P. M.; Rowland, R. S.; Taylor, R.; Verdonk, M. L. IsoStar: A library of information about nonbonded interactions. *J. Comput. Aided Mol. Des.* **1997,** *11*, 525-537.
(26) Lentijo, S.; Miguel, J. A.; Espinet, P. Highly fluorescent platinum(II) organometallic complexes of perylene and perylene monoimide, with Pt σ-bonded directly to the perylene core. *Inorg. Chem.* **2010,** *49*, 9169-9177.

(27) Wang, J. P.; Niu, C. J.; Hu, N. H. Heptaaquatetra-μ_3-hydroxy-hexa-μ_2-L-leucine-(L-leucine)tetraytterbium(III) tetrachlorozinc(II) trichlorohydroxyzinc(II) tetrachloride octahydrate. *Acta Cryst. Section C* **2004,** *60*, M143-M146.
(28) Cotton, S. A.; Franckevicius, V.; Mahon, M. F.; Ooi, L. L.; Raithby, P. R.; Teat, S. J. Structures of 2,4,6-tri-alpha-pyridyl-1,3,5-triazine complexes of the lanthanoid nitrates: A study in the lanthanoid contraction. *Polyhedron* **2006,** *25*, 1057-1068.
(29) Yoshida, M.; Khokhar, A. R.; Siddik, Z. H. Axial ligands and alicyclic ring size modulate the activity and biochemical pharmacology of ammine cycloalkylamine-platinum(IV) complexes in tumor-cells resistant to cis-diamminedichloroplatinum(II) or trans-1R,2R-1S,2S-diaminocyclohexanetetrachloroplatinum(IV). *Cancer Res.* **1994,** *54*, 4691-4697.
(30) Kisova, A.; Zerzankova, L.; Habtemariam, A.; Sadler, P. J.; Brabec, V.; Kasparkova, J. Differences in the cellular response and signaling pathways between cisplatin and monodentate organometallic Ru(II) antitumor complexes containing a terphenyl ligand. *Mol. Pharmaceutics* **2011,** *8*, 949-957.
(31) Ormerod, M.; O'Neill, C.; Robertson, D.; Kelland, L.; Harrap, K. cis-Diamminedichloroplatinum(II)-induced cell death through apoptosis in sensitive and resistant human ovarian carcinoma cell lines. *Cancer Chemother. Pharmacol.* **1996,** *37*, 463-471.
(32) Liskova, B.; Zerzankova, L.; Novakova, O.; Kostrhunova, H.; Travnicek, Z.; Brabec, V. Cellular response to antitumor cis-dichlorido platinum(II) complexes of CDK inhibitor bohemine and its analogues. *Chem. Res. Toxicol.* **2012,** *25*, 500-509.
(33) Brabec, V.; Palecek, E. Interaction of nucleic acids with electrically charged surfaces. II. Conformational changes in double-helical polynucleotides. *Biophys. Chem.* **1976,** *4*, 76-92.
(34) Brabec, V.; Palecek, E. The influence of salts and pH on polarographic currents produced by denatured DNA. *Biophysik* **1970,** *6*, 290-300.
(35) Dhara, S. C. Process for the production of pure cis-platinum-(II)-idiammine dichloride. *Indian J. Chem.* **1970,** *8*, 193-194.
(36) Burla, M. C.; Caliandro, R.; Camalli, M.; Carrozzini, B.; Cascarano, G. L.; De Caro, L.; Giacovazzo, C.; Polidori, G.; Spagna, R. SIR2004: an improved tool for crystal structure determination and refinement. *J. Appl. Crystallogr.* **2005,** *38*, 381-388.
(37) Sheldrick, G. M. A short history of SHELX. *Acta Crystallogr. Sect. A* **2008,** *64*, 112-122.
(38) Nardelli, M. Parst: A system of fortran routines for calculating molecular structure parameters from results of crystal structure analyses. *Comput. Chem.* **1983,** *7*, 95-98.
(39) Nardelli, M. PARST95 – an update to PARST: a system of Fortran routines for calculating molecular structure parameters from the results of crystal structure analyses. *J. Appl. Crystallogr.* **1995,** *28*, 659-659.
(40) Farrugia, L. J. WinGX suite for small-molecule single-crystal crystallography. *J. Appl. Crystallogr.* **1999,** *32*, 837-838.
(41) Farrugia, L. J. ORTEP-3 for Windows - a version of ORTEP-III with a Graphical User Interface (GUI). *J. Appl. Crystallogr.* **1997,** *30*, 565-565.
(42) Egger, A. E.; Rappel, C.; Jakupec, M. A.; Hartinger, C. G.; Heffeter, P.; Keppler, B. K. Development of an experimental protocol for uptake studies of metal compounds in adherent tumor cells. *J. Anal. Atom. Spectrom.* **2009,** *24*, 51-61.
(43) Brabec, V.; Leng, M. DNA interstrand cross-links of trans-diamminedichloroplatinum(II) are preferentially formed between guanine and complementary cytosine residues. *Proc. Natl. Acad. Sci. USA* **1993,** *90*, 5345-5349.
(44) Moser, C.; Lang, S. A.; Kainz, S.; Gaumann, A.; Fichtner-Feigl, S.; Koehl, G. E.; Schlitt, H. J.; Geissler, E. K.; Stoeltzing, O. Blocking heat shock protein-90 inhibits the invasive properties and hepatic growth of human colon cancer cells and improves the efficacy

of oxaliplatin in p53-deficient colon cancer tumors in vivo. *Mol. Cancer Ther.* **2007,** *6,* 2868-2878.